Diffuse xray scattering study of toluene and polybromostyrene PBrS/toluene solutions

W. Zhao, X. Zhao, J. Sokolov, M. H. Rafailovich, M. K. Sanyal et al.

Citation: J. Chem. Phys. **97**, 8536 (1992); doi: 10.1063/1.463371
View online: http://dx.doi.org/10.1063/1.463371
View Table of Contents: http://jcp.aip.org/resource/1/JCPSA6/v97/i11
Published by the American Institute of Physics.

Diffuse x-ray scattering study of toluene and polybromostyrene PBrS/toluene solutions

W. Zhao, X. Zhao, J. Sokolov, and M. H. Rafailovich
Department of Physics, Queens College, Flushing, New York 11367

M. K. Sanyal[a] and S. K. Sinha[b]
Physics Department, Brookhaven National Laboratory, Upton, New York 11973

B. H. Cao
Exxon Research and Engineering Company, Annandale, New Jersey 08801 and Department of Physics, City College of CUNY, New York, New York, 10031

M. W. Kim
Exxon Research and Engineering Company, Annandale, New Jersey 08801

B. B. Sauer
E. I. Du Pont de Nemours and Company, Inc., Experimental Station, Wilmington, Delaware 19898

(Received 14 May 1992; accepted 20 August 1992)

We report measurements and calculations of x-ray diffuse scattering from the liquid–vapor interface of toluene and polybromostyrene(PBrS)/toluene solutions for polymer molecular weights 90 K and 1 M at concentrations up to 11.7 volume %, well into the entangled semidilute regime. We have calculated the static structure factor $S(k)$ and equal time height–height correlation function $C(R)$ for surface hydrodynamic modes based on a coupled two-fluid model where the polymer response is taken to be that of a Maxwell viscoelastic material [Harden *et al.*, J. Chem. Phys. **94**, 5208 (1991)]. We obtain the leading correction term to the capillary-wave result for $C(R)$ dependent on the solution shear modulus E_0, as well as an analytic approximation valid for large E_0, including the case of pure polymer melt.

I. INTRODUCTION

Liquid polymers and polymer solutions exhibit complex non-Newtonian hydrodynamic behavior as a result of interchain entanglements and much theoretical and experiment work[1–4] has been done in order to understand the bulk properties of these materials. Obtaining information on the corresponding surface properties has been hindered by the lack of sufficiently surface-sensitive experimental probes. However, recent developments in light-scattering[5] and x-ray scattering techniques[6–9] have made it possible to study surface hydrodynamic modes on liquids. In addition, several authors have recently made model calculations[10,11] of surface mode dispersion relations and structure factors for complex liquids which take account of the properties of viscoelasticity and surface tension. We report here diffuse x-ray scattering measurements from toluene and polybromostyrene(PBrS)/toluene solutions for polymer concentrations up to 11.7 volume %, well into the entangled regime for the two molecular weights studied, 90 K and 1 M.

II. EXPERIMENTAL SECTION

The samples used for this study were the pure solvent toluene and solutions of toluene and polybromostyrene (PBrS). The PBrS was prepared by solution bromination of narrow distribution parent batches of polystyrene (90 K, Mw/Mn=1.04 and 1 M, Mw/Mn$\leqslant$1.10, purchased from Polymer Labs) according to the prescription of Kambour and Bendler.[12] Bromination levels, typically 0.9 Br atoms per styrene monomer, were determined by mass microanalysis. Toluene is a good solvent for PBrS and from consideration of the corresponding surface tension, 27.7 dyn/cm for toluene, 39.5 dyn/cm for pure PBrS, the near surface region is expected to be partially depleted of the polymer component.

The x-ray diffuse scattering measurements were made using the liquid spectrometer on beamline X22B[13] of the Brookhaven National Synchrotron Light Source. The sample cell was a temperature-controlled closed chamber with beam entrance and exit windows which could hold 3 in. diam polished silicon wafers (Semiconductor Processing, Boston, MA) used as substrates. Approximately 2 ml of each solution was deposited by pipette onto the substrates, forming layers thick enough, about 400 μm, so that scattering from the silicon/solution interface was negligible. A reservoir of toluene was maintained in the cell and the sample thickness was monitored to check that the solution was stable during the course of the experiment.

Figure 1 shows the scattering geometry of the x-ray experiment. The momentum transfer vector is $\mathbf{q}\equiv\mathbf{k}_s-\mathbf{k}_i$, where $\mathbf{k}_i$ and $\mathbf{k}_s$ are the incident and scattered wave vectors, respectively, making angles α and β with respect to the macroscopic liquid surface. The z direction is taken normal to the sample surface while the projection of the incident

[a]On leave from Solid State Physics Division, Bhabha Atomic Research Center, Bombay-400 085, India.
[b]Also at Corporate Research Laboratories, Exxon Research and Engineering, Annandale, New Jersey 08801.

 0021-9606/92/238536-07$006.00

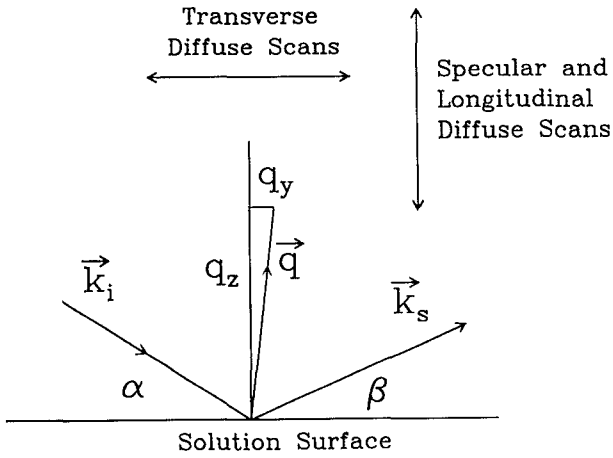

FIG. 1. Scattering geometry of the x-ray experiment, showing incident and scattered wave vectors, $\mathbf{k}_i$ and $\mathbf{k}_s$ relative to the macroscopic sample surface.

wave vector $\mathbf{k}_i$ on the surface is used to define the y direction. Specular scans are intensity vs angle (or q_z) spectra where α is varied, maintaining $\alpha=\beta$, i.e., $q_x=q_y=0$ and $q_z=(4\pi/\lambda)\sin\alpha$. Nonspecular, or diffuse, scans can be collected in a variety of ways depending on the experimental setup. We have used the following two types: (1) transverse diffuse scans, where q_z is fixed and q_y is varied, and (2) longitudinal diffuse scans, where q_y is fixed at some nonzero value and q_z is varied (see Fig. 1). The intensity measured in a specular scan, due to the finite instrumental resolution, includes a contribution from the experimentally inseparable diffuse scattering at the vicinity of the specular condition $\alpha=\beta$. The specular reflectivity thus measured is mostly sensitive to variations in electronic density in the direction normal to the surface and the average roughness of the liquid–vapor interface (static and fluctuations). It has been shown[6–9,14] that the specular reflectivity has the form $R(q_z)=e^{-q_z^2\sigma_{\text{eff}}^2}R_F(q_z)$, where R_F is the corresponding Fresnel reflectivity from a smooth surface and σ_{eff}^2 is an effective roughness which depends on the density profile, roughness and the instrumental resolution. If the resolution function is known, the intrinsic surface roughness may be extracted. The intensity of the diffuse scattering is sensitive to surface fluctuations, as will be discussed below, and is therefore a useful probe for helping to answer the question of what proportions of the polymer solution liquid–vacuum interface are due to static roughness, fluctuations, or density gradients and when is uniquely polymerlike behavior to be expected.

Specular and diffuse spectra were recorded for the solvents and polymer solutions listed in Table I. Typical specular scans were from q_z equal to 0.02 to 0.4 Å^{-1}, longitudinal diffuse scans for q_z from 0.052 to 0.3 Å^{-1} with $q_y=0.0005$ Å^{-1} (near the specular direction, but outside the resolution half-width) and transverse diffuse scans for $q_y\cong -2\times10^{-3}$ Å^{-1} to 2×10^{-3} Å^{-1} for fixed q_z of 0.10, 0.15, 0.20, 0.25, and 0.30 Å^{-1}. The X22B monochromator consists of a focussing cylindrical mirror followed by a single Ge(111) crystal scattering in a horizontal geometry. The

TABLE I. Relaxation times, fitting constants, shear moduli, and values of the first-order correction term to $C(R)$ for the solutions studied.

	τ(s)	$c(\tau)$	E_0(dyn/cm^2)	$\pi c(\tau)E_0/4\gamma\kappa$
90 K 3.18%	1.6×10^{-6}	$\sim5\times10^{-5}$	747	6×10^{-4}
11.7%	1.1×10^{-5}	$\sim5\times10^{-5}$	1400	1×10^{-2}
1 M 1.9%	9.9×10^{-4}	$\sim1.5\times10^{-4}$	234	5.0×10^{-4}
3.39%	2.35×10^{-3}	$\sim2\times10^{-4}$	862	2.5×10^{-3}

incident beam energy was set to 8 keV. The scattering plane was vertical with the beam slits defining the incident beam in the vertical set to be 0.2 mm and in the horizontal to be 0.4 mm. Two sets of exit slits were used: guard slits to reduce stray background scattering, located approximately 15 cm from the sample and set at 1 mm vertical by 5 mm horizontal and detector slits, located immediately in front of the NaI scintillation detector set at 0.5 mm vertical by 5 mm horizontal. This slit geometry essentially integrates the intensity in the q_x direction and simplifies the analysis.[7,8] Detector 2θ scans through the unscattered incident beam had FWHM angular widths of 0.05° (0.8 mrad). Data acquisition times for transverse diffuse scans ranged from about 20 min at $q_z=0.10$ Å^{-1} to 2 h at $q_z=0.30$ Å^{-1}.

III. ANALYSIS

Recent diffuse x-ray scattering experiments from small-molecule liquids, such as ethanol[8] and water,[15] have been successfully interpreted using a capillary wave model for the surface fluctuations. For weak scattering, reflectivity $R\ll1$, it can be shown[7] that the differential cross section for scattering in the distorted wave born approximation is given by

$$\frac{d\sigma}{d\Omega}=A\frac{q_c^4}{16\cdot\pi^2}|T(\mathbf{k}_i)|^2|T(\mathbf{k}_s)|^2\frac{1}{q_z^2}\times\int e^{-i\mathbf{q}_\parallel\cdot\mathbf{R}}e^{-q_z^2C(\mathbf{R})}d\mathbf{R}, \quad (1)$$

where A is the area of the sample illuminated by the beam, q_c is the critical wave vector for total reflection, $T(\mathbf{k}_i)$ and $T(\mathbf{k}_s)$ are Fresnel transmission coefficients, $\mathbf{q}_\parallel=(q_x,q_y)$ is the in-plane part of the scattering wave vector $\mathbf{q}$, $C(\mathbf{R})$ is the equal-time direct space height–height correlation function for the liquid surface ($C(\mathbf{R})=C(R)$) for an isotropic surface), $\mathbf{R}$ is the distance vector in the surface plane and we have taken $q\gg q_c$ so that q_z may be evaluated from the external $\mathbf{k}_i$ and $\mathbf{k}_s$. The experimentally measured intensity I is obtained by folding this cross section with the instrumental resolution in q space. For purely capillary–gravity fluctuations, a specific analytic form is given in Ref. 8. Therefore, the main ingredient of a diffuse scattering calculation is an evaluation of $C(R)$, which is determined by the types of surface vibrational modes present. Pure polymers and polymer solutions have surface modes which differ in character from those found in small-molecule liquids due to the well-known viscoelastic behavior of polymers.[2,16] The material response of viscoelastic substances

to low-frequency disturbances is primarily that of a viscous liquid while their response to high-frequency disturbances is primarily that of an elastic solid. The crossover between these two regimes can be characterized approximately by a single crossover frequency ω_c and relaxation time $\tau \sim 1/\omega_c$, though real systems may have a broad crossover and a spectrum of relaxation times. An interpolation scheme, due to Maxwell,[16] is to model the material with a frequency-dependent complex shear modulus $E(\omega)=iE_0\omega\tau/(1+i\omega\tau)$, where ω is the frequency, τ is the relaxation time, and E_0 the transient modulus of the polymer solution. For $\omega \gg 1/\tau$, the solution will respond as an elastic solid with modulus E_0 and for $\omega \ll 1/\tau$ will behave as a viscous liquid of viscosity $\eta \sim E_0\tau$. Harden *et al.*[10] have considered a coupled two-fluid model of polymer solutions, where the polymer response is of the Maxwell form. In the perfect coupling limit of Ref. 10, where the local polymer and solvent velocities are equal, the coupled equations of motion for the polymer and solvent reduce to a single equation for the responses of both solvent (purely viscous) and polymer (Maxwell viscoelastic). Their result for the dynamic structure factor [$S(k,\omega) \equiv$ the time and space Fourier transform of the height–height correlation function] due to thermally excited hydrodynamic surface modes is

$$S(k,\omega)=\frac{8k_BT\,\mathrm{Re}[\eta(\omega)]k^3}{\rho^2|D(k,\omega)|^2}\left(1+\frac{1}{2\,\mathrm{Re}[\alpha(k,\omega)]}-2\,\mathrm{Re}\left[\frac{1}{1+\alpha(k,\omega)}\right]\right), \tag{2}$$

where k_B represents Boltzmann's constant, T represents temperature, k represents wave vector, ω represents frequency, $\eta(\omega)=\eta_0+E(\omega)/i\omega$ is the frequency-dependent viscosity of the viscoelastic polymer plus solution, η_0 =solvent viscosity, $E(\omega)$ is as given above, ρ=mass density of fluid,

$$D(k,\omega)=[i\omega+2\nu(\omega)k^2]^2-4\nu(\omega)^2k^4\left(1+\frac{i\omega}{\nu(\omega)k^2}\right)^{1/2}+\frac{\gamma k^3}{\rho}, \tag{3}$$

where $D(k,\omega)=0$ gives the dispersion relation for the medium, $\nu(\omega)=\eta(\omega)/\rho$, γ=solution surface tension and

$$\alpha(\omega)\equiv\left(1+\frac{i\omega}{\nu(\omega)k^2}\right)^{1/2}. \tag{4}$$

The x-ray scattering experiments, due to the energy of typical hydrodynamic excitations (~meV and less) being negligible compared to the energy resolution of the experiment (~few eV), effectively integrate over ω and are sensitive only to the static structure factor $S(k)\equiv(1/2\pi)\int_{-\infty}^{\infty} S(k,\omega)d\omega$, which is the space Fourier transform of the equal-time height–height correlation function. In the large k (capillary wave) limit, it can be shown that $S(k)\to S_{\mathrm{cap}}(k)=k_BT/\gamma k^2$ while in the small k (elastic) limit $S(k)\to S_{\mathrm{elastic}}(k)=k_BT/cE_0k$, where c is a constant of order 1. An interpolation formula between these limits, suggested by the fact that the surface energy/area in a combined elastic+capillary mode can be approximated as $E(E_0,\gamma,k)\cong\gamma k^2/4+c'E_0k$, c' a constant, is

$$S(k)\cong\frac{k_BT}{\gamma k^2+c(\tau)E_0k}, \tag{5}$$

where use has been made of the equipartition theorem. The $S(k,\omega)$ of Harden *et al.* was numerically integrated and fit to the form of Eq. (5), with $c(\tau)$ the only fitting parameter. The results are shown in Figs. 2–4 and it can be seen that this form of $S(k)$ well represents the numerically calculated $S(k)$. The value of $c(\tau)$ is found to be independent of E_0 (see Fig. 3). The τ dependence is shown in Fig. 5, $c(\tau)$ increases as τ increases and $c(\tau)$ asymptotically approaches the value 2 for τ greater than a few seconds, in agreement with the result for a purely elastic material.[11] Finally, we add in the effects of gravity approximately in such a way as to reduce to the known capillary+gravity result[8] for $E_0=0$

$$S(k)\cong\frac{k_BT}{\gamma(k^2+\{[c(\tau)E_0k]/\gamma\}+\kappa^2)}, \tag{6}$$

where $\kappa=(\rho g/\gamma)^{1/2}$ is the long-wavelength gravitational cutoff with ρ=liquid mass density and g=gravitation constant=980 cm/s^2. This analytic form of $S(k)$ can be conveniently used to make diffuse scattering calculations along the lines of Ref. 7. However, we must first back-transform $S(k)$ to give the real space height–height correlation function, i.e.,

$$C(R)=\frac{1}{(2\pi)^2}\int S(k)e^{-i\mathbf{k}\cdot R}\,d\mathbf{k}, \tag{7}$$

where the integration is taken over the whole k plane in order to obtain a closed-form expression (that is, $k_{\min}=2\pi/\lambda_{\max}$, where $\lambda_{\max}\sim$sample size$\sim$cm and $k_{\max}=2\pi/\lambda_{\min}$, $\lambda_{\min}\sim$interatomic spacing $\sim$Å are set to 0 and ∞, respectively). Since $S(k)$ does not depend on the direction of $\mathbf{k}$, we may use polar coordinates and integrate over the angular variable to obtain

$$C(R)=\frac{1}{2\pi}\int_0^\infty dk\,kJ_0(kR)\cdot S(k)=\frac{k_BT}{2\pi\gamma}\int_0^\infty dk\,\frac{kJ_0(kR)}{k^2+\{[c(\tau)E_0k/\gamma\}+\kappa^2}. \tag{8}$$

The term in the integrand multiplying $J_0(kR)$ can be factored

$$\frac{k}{k^2+\frac{c(\tau)E_0k}{\gamma}+\kappa^2}=\frac{d_1}{k-r_1}+\frac{d_2}{k-r_2}, \tag{9}$$

$$r_{1,2}=\frac{1}{2}\left(\frac{-c(\tau)E_0}{\gamma}\pm\sqrt{\left(\frac{c(\tau)E_0}{\gamma}\right)^2-4\frac{g\rho}{\gamma}}\right)\equiv\frac{1}{2}\left(-\frac{c(\tau)E_0}{\gamma}\pm\beta\right),$$

$$d_1=\frac{r_1}{r_1-r_2}=\frac{1}{2}\left(1-\frac{c(\tau)E_0}{\gamma\beta}\right),$$

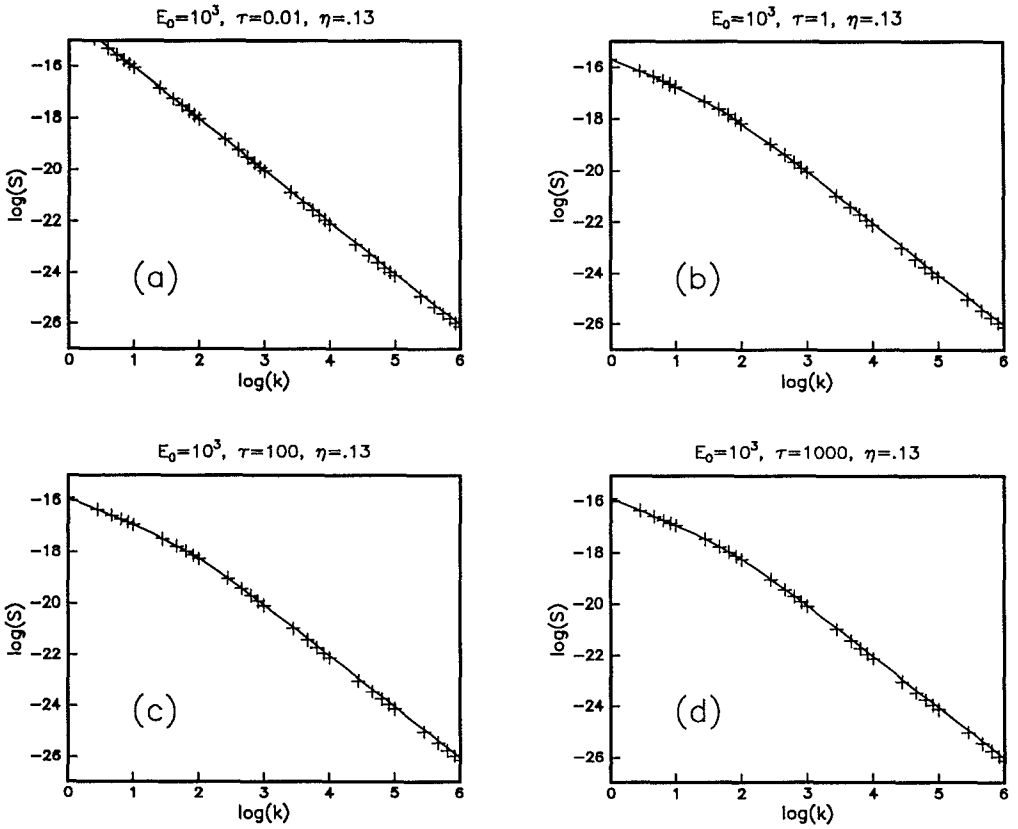

FIG. 2. Static structure face $S(k)$ obtained by numerically integrating Eq. (1),—compared with the fit to the analytic form of Eq. (4), $+++$. Variation with τ is shown. (a) is nearly completely capillary wavelike. Units of E_0 are dyn/cm^2, τ seconds, η poise, and k cm^{-1}.

$$d_2=1-d_1=\frac{1}{2}\left(1+\frac{c(\tau)E_0}{\gamma\beta}\right). \tag{10}$$

We make use of the integral,[17]

$$\int_0^\infty \frac{J_0(kR)dk}{k-r_1}=\frac{\pi}{2}\left[H_0(-r_1R)-N_0(-r_1R)\right], \tag{11}$$

where $H_0(x)$ is a Struve function and $N_0(x)$ is a Neumann function to write

$$C(R)=\frac{k_BT}{2\pi\gamma}\cdot\frac{\pi}{2}\left[d_1[H_0(-r_1R)-N_0(-r_1R)]\right.$$
$$\left.+d_2[H_0(-r_2R)-N_0(-r_2R)]\right]. \tag{12}$$

This expression may be simplified by noting that $|-r_{1,2}R|$ is small for $R\ll L$ (where L=x-ray coherence length parallel to the surface, $\cong 10^{-3}$ cm) and using the small argument expansions[18] for H_0, N_0, i.e., $H_0(z)\cong(2/\pi)z$ and $N_0(z)\cong(2/\pi)[\ln(z/2)+\gamma_E]$, with $\gamma_E=0.5772$. Further, we take $c(\tau)E_0\lesssim 10^3$ dyns/cm^2, which makes β of Eq. (10) purely imaginary. The result is

$$C(R)\cong\frac{k_BT}{2\pi\gamma}\left[-\ln\left(\frac{\kappa R}{2}\right)-\gamma_E-\frac{\pi c(\tau)E_0}{4\gamma\kappa}\right]. \tag{13}$$

The last term is a correction term to the capillary-plus-gravity wave result,[8] linearly dependent on E_0 and dependent on the polymer relaxation time τ though $c(\tau)$. Since the correction term in this limit is only an additive constant to $C(R)$, the diffuse scattering lineshape (intensity vs q_y) remains unchanged. This will not be true for values of $E_0\gtrsim 10^5$ dyns/cm^2 for which case terms linear in R and higher order must be added to Eq. (13). We have obtained values of τ and E_0 from independent surface light scattering experiments[19] for the high concentration, 11.7 volume %, PBrS/toluene solution. The values for the other solutions studied were estimated using the scaling prediction[4,20] $\tau\sim(\mathrm{Mw})^3\cdot\phi^{3/2}$, where ϕ is the polymer concentration. The results are shown in Table I, with the τ and E_0 estimates found to be comparable to those derived from the mechanical measurements of Adam and Delsanti[21] on PS/benzene solutions. It can be seen in Table I that the E_0-dependent term in Eq. (13) is negligible for all cases in the table. Therefore, we expect that the diffuse scattering will be dominated by capillary-wave effects and we use the small-molecule liquid calculations of Refs. 7 and 8. The surface tension γ of each solution was measured with a modified Wilhelmy technique[22] and found to be equal, within experimental error, to the pure toluene value of 27.7 dyn/cm. The comparison between the calculated and experimental spectra is shown in Figs. 6(a)–6(c). The overall agreement for the polymer solutions is comparable to that obtained for the pure solvent toluene. Apart from a constant concentration-dependent background (due to bulk scattering), the spectra are the same as for toluene, consistent with Eq. (12) and Table I which show that even though the polymer solutions are well into the entangled

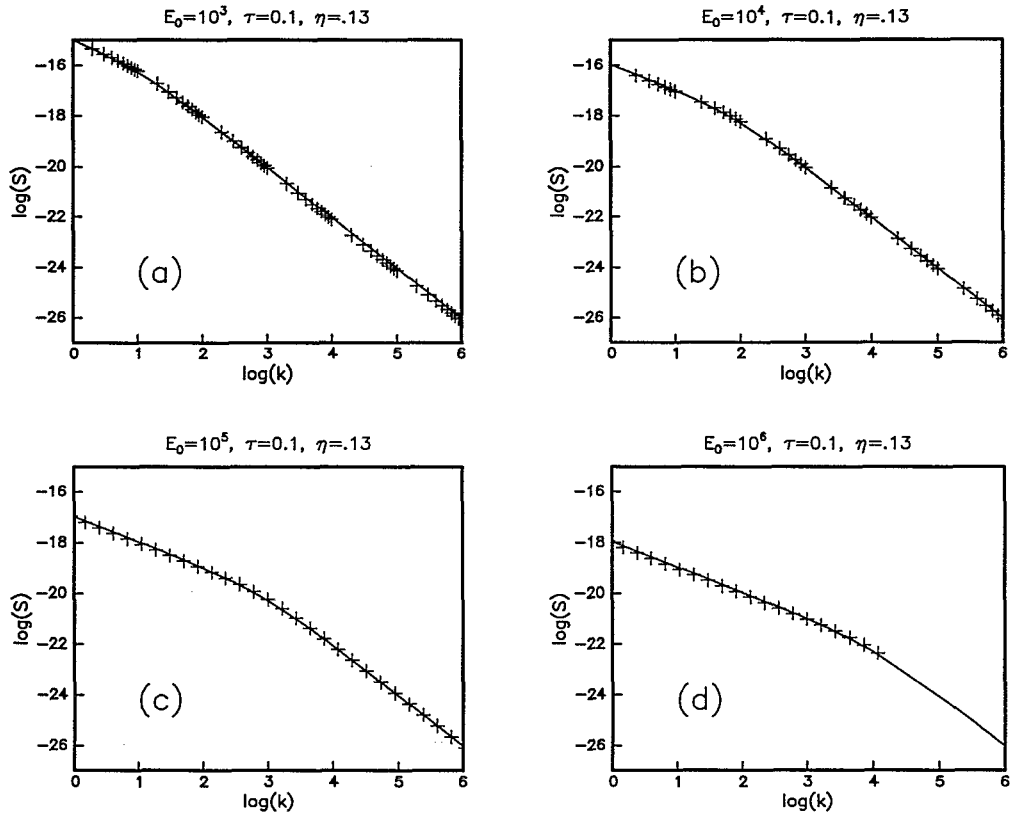

FIG. 3. As in Fig. 2, but showing the variation with shear modulus E_0.

semidilute regime the diffuse spectra are largely unaffected. The root-mean-square fluctuation, σ, is 5.1 ± 0.2 Å. Also shown is a comparison of experimental data for the solvent chlorobenzene and a 15% PDMS(Mw=1 M)/chlorobenzene solution. This system was chosen because the electronic densities of solvent and polymer are well matched (0.344 e/Å^3 for chlorobenzene, 0.324 e/Å^3 for PDMS) and therefore the bulk background scattering is greatly reduced compared to the PBrS/toluene system (electronic density of PBrS is 0.465 e/Å^3, toluene 0.283 e/Å^3). Also, the PDMS is expected to strongly segregate to the solution surface since the surface tension of PDMS is 20.5 dyn/cm vs 33 dyn/cm for chlorobenzene. This system is opposite to the PBrS/toluene case, where the surface is polymer depleted, and provides a test of our assumption

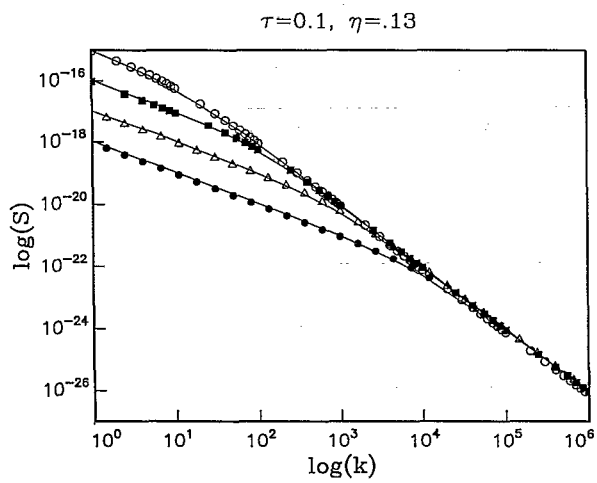

FIG. 4. As in Fig. 3, superposed on one plot: ●, $E_0=10^6$ dyn/cm^2; △, $E_0=10^5$ dyn/cm^2; ■, $E_0=10^4$ dyn/cm^2; ○, $E_0=10^3$ dyn/cm^2.

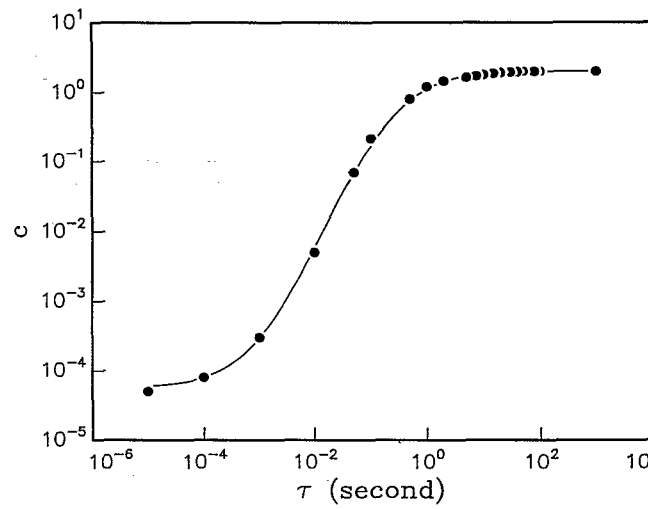

FIG. 5. Dependence of the fitting parameter $c(\tau)$ of Eq. (4) on the Maxwell relaxation time τ.

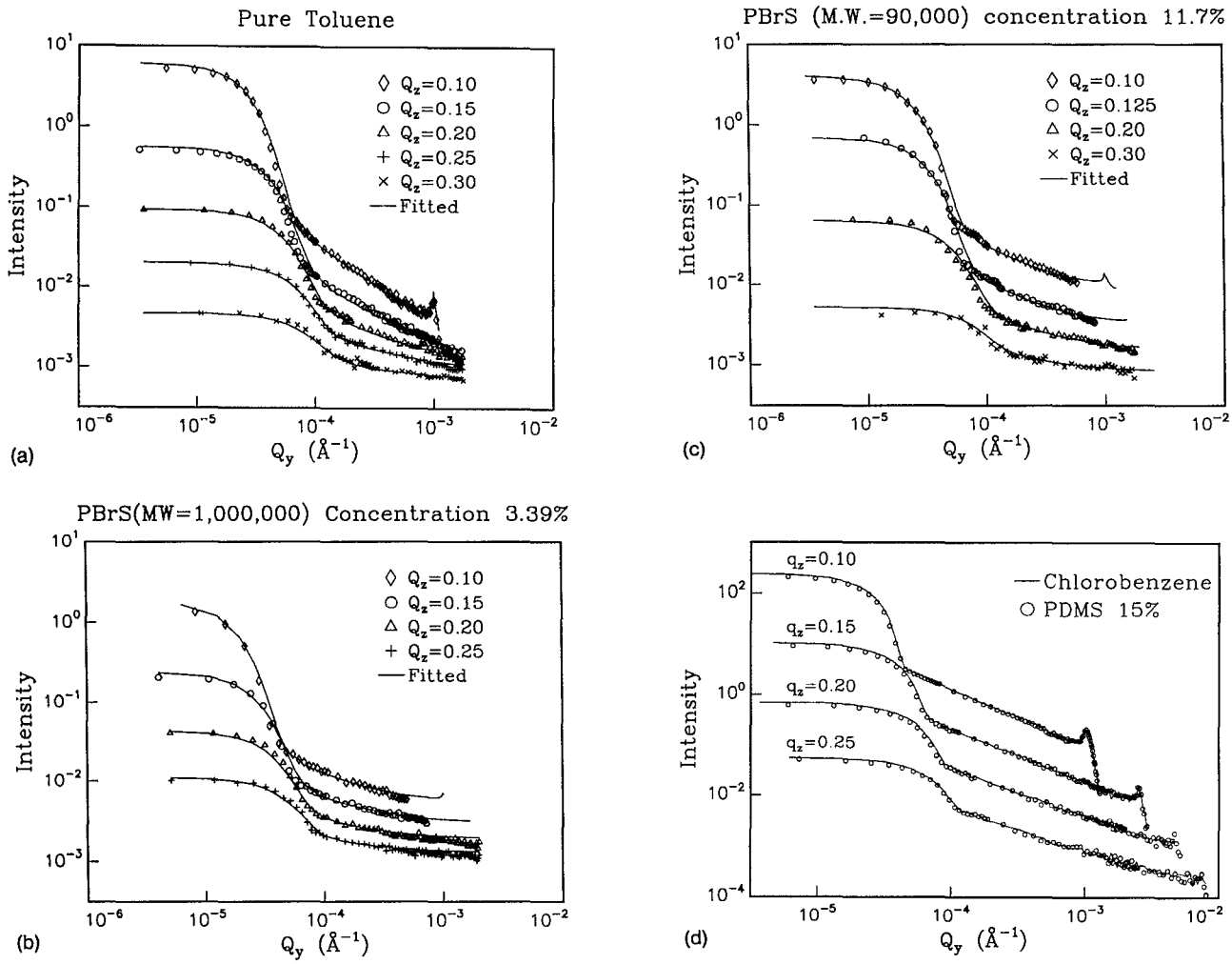

FIG. 6. Diffuse scattering spectra for toluene and polymer solutions. The smooth curves in (a)–(c) are capillary wave model calculations. Part (d) shows experimental curves for pure chlorobenzene and a 15% PDMS/chlorobenzene solution. Units of Q_z are Å^{-1}.

that the surface modes may be calculated for solutions having constant bulk density profiles (this assumption is based on the observation that the wavelengths and penetration depths of most of the surface modes are much greater then the widths of the surface depletion or segregation regions—a fews tens of Ångstoms—and therefore the dynamics of the surface modes should be largely unaffected). The experimental data are shown in Fig. 6(d), without any background corrections, for pure solvent and a 15% PDMS solution. The small decrease in scattering for the solution compared to chlorobenzene can be accounted for by the reduction in surface tension to 27.1 dyn/cm for solution. Capillary wave calculations using the measured surface tension for solvent and solution give good fits, with no need to invoke the effects of elasticity.

IV. CONCLUSIONS

We have made calculations of the static structure factor $S(k)$ and height–height correlation function $C(R)$ for surface hydrodynamic modes of polymer solutions based on a coupled two-fluid model[10] with Maxwell viscoelastic response for the polymer. These calculations indicate that even for solutions well into the semidilute regime the behavior of $S(k)$ is capillary wavelike for most of the range of k values sampled in a typical x-ray scattering experiment, $\sim 10^3 \rightarrow 10^8$ cm^{-1}. Experiments on semi-dilute solutions of PBrS/toluene and PDMS/chlorobenzene confirm this picture. The calculations further show that in order to observe with x-rays significant effects due to the elasticity of polymers, one must study highly concentrated solutions or melts. This is the subject of current investigations.

ACKNOWLEDGMENTS

We would like to thank J. Harden and R. Kambour for many helpful discussions. This work was supported in part by the Department of Energy (DE-FG02-90ER45437), the National Science Foundation (DMR-8921556) and the Petroleum Research Fund of the American Chemical Society (23547-AC7-SF92).

[1] R. B. Bird, C. F. Curtiss, R. C. Armstrong, and O. Hassager, *Dynamics of Polymeric Liquids*, Vols. 1 and 2, 2nd ed. (Wiley, New York, 1987).
[2] J. D. Ferry, *Viscoelastic Properties of Polymers*, 3rd ed. (Wiley, New York, 1980).

[3] M. Doi and S. F. Edwards, *The Theory of Polymer Dynamics* (Oxford University, New York, 1986).
[4] P.-G. de Gennes, *Scaling Concepts in Polymer Physics* (Cornell University, Ithaca, New York, 1979).
[5] H. Z. Cummins and H. L. Swinney, Prog. Opt. **8**, 133 (1970); B. B. Sauer, M. Kawaguchi, and H. Yu, Macromolecules **20**, 2732 (1987); B. H. Cao, M. W. Kim, H. Schaeffer, and H. Z. Cummins, J. Chem. Phys. **95**(12), 9317 (1991).
[6] A. Braslau, M. Deutsch, P. S. Pershan, A. H. Weiss, J. Als-Nielsen, and J. Bohr, Phys. Rev. Lett. **54**, 114 (1985).
[7] S. K. Sinha, E. B. Sirota, S. Garoff, and H. B. Stanley, Phys. Rev. B **88**, 2297 (1988).
[8] M. S. Sanyal, S. K. Sinha, K. G. Huang, and B. M. Ocko, Phys. Rev. Lett. **66**, 628 (1991).
[9] J. Als-Nielsen, in *Structure and Dynamics of Surfaces II: Topics in Current Physics*, Vol. 43, edited by W. Schommers and P. van Blanckenhagen (Springer-Verlag, Berlin, 1987), p. 181.
[10] H. Pleiner, J. L. Harden, and P. Pincus, Europhys. Lett. **7**, 383 (1988); J. L. Harden, H. Pleiner, and P. A. Pincus, J. Chem. Phys. **94**, 5208 (1991).
[11] G. H. Fredrickson, A. Ajdari, L. Leibler, and J.-P. Carton, Macromolecules (in press).
[12] R. T. Kambour and J. T. Bendler, Macromolecules **19**, 2679 (1986).
[13] J. Als-Nielsen and P. S. Pershan, Nucl. Instr. Methods **208**, 545 (1983).
[14] A. Braslau, P. S. Pershan, G. Swislow, B. M. Ocko, and J. Als-Nielsen, Phys. Rev. A **38**, 2457 (1988).
[15] D. K. Schwartz, M. L. Schlossman, E. H. Kawamoto, G. J. Kellogg, P. S. Pershan, and B. M. Ocko, Phys. Rev. A **41**, 5687 (1990).
[16] N. W. Tschoegl, *The Phenomenological Theory of Linear Viscoelastic Behavior* (Springer-Verlag, Berlin, 1988).
[17] I. S. Gradshteyn and I. M. Ryzhik, *Table of Integrals, Series and Products* (Academic, New York, 1980), p. 685.
[18] *Handbook of Mathematical Functions*, edited by M. Abramowitz and I. A. Stegun (Dover, New York, 1965), pp. 360 and 496.
[19] B. H. Cao and M. W. Kim (unpublished).
[20] P.-G. de Gennes, Macromolecules **9**, 587 (1976).
[21] M. Adam and M. Delsanti, J. Phys. **44**, 1185 (1983).
[22] B. B. Sauer and N. V. Dipaolo, J. Colloid Interface Sci. **144**, 527 (1991).